Strojniški vestnik - Journal of Mechanical Engineering 70(2024)11-12, pp1-pp13
DOI:10.5545/sv-jme.2024.1072
Original Scientific Paper
Received for review: 2024-06-24
Received revised form: 2024-09-14
Accepted for publication: 2024-09-18

Gear Differential Flank Modification Design Method for Low Noise

Yu Zhang[1,2,*] – Hai Zhou[1,2] – Chengyu Duan[1,2] – Zhiyong Wang[1,2] – Hong Luo[1,2]

[1] Central South University of Forestry and Technology, Institute of Modern Mechanical Transmission Engineering Technology, China

[2] Central South University of Forestry and Technology, Engineering Research Center for Forestry Equipment of Hunan Province, China

To address the limitations of existing gear tooth modification methods, a differentiated tooth modification method is proposed, where the modification amount of adjacent teeth varies according to a sine function. Initially, a mathematical model of the gear tooth profile varying according to a sine function is established. Then, using Adams software, a simulation analysis of the dynamic characteristics such as centroid angular acceleration, meshing force, and transmission error of gear pairs is conducted. The dynamic transmission performance of three sets of gear pairs—unmodified, normally modified, and differentially modified—is compared. Additionally, Simcenter 3D software is used to analyze the noise characteristics of these gear pairs. The results show that the differentially modified gear pairs, compared to the normally modified ones, have a maximum reduction of 2.47 % in sound power level at the fundamental meshing frequency amplitude. This proves that the differentiated modification method enhances the dynamic transmission performance of gears, offering a new method for gear vibration and noise reduction.

Keywords: tooth modification; low noise; angular acceleration; meshing force

Highlights

- *A gear modification method is proposed with modifications varying by a sine function.*
- *A mathematical model for tooth profiles varying sinusoidally has been established.*
- *This method reduces angular acceleration, meshing force, and transmission error.*

0 INTRODUCTION

Gear transmission is one of the core components in automobiles, and its performance directly affects the comfort and safety of the passengers [1] to [3]. Currently, electrification represents the main trend in automotive development. The most significant difference between electric vehicles (EVs) and traditional internal combustion engine vehicles lies in the power system. The replacement of the engine with an electric motor has a profound impact on the gear transmission system, leading to the development of reducers that are higher revolutions per minute (RPM), more efficient, and capable of handling higher peak torques. The maximum input speed of these reducers has reached 15,000 rpm to 20,000 rpm, even higher, which is 3 to 10 times higher than that of traditional vehicles. Consequently, the noise generated by the gear transmission system during high-speed engagement has become a major source of noise in EVs [4] to [6]. Moreover, unlike internal combustion vehicles, electric vehicles lack engine noise to mask other sounds, making the noise from the reducer assembly more pronounced. The noise quality of EVs can even be worse than that of traditional vehicles, significantly reducing the noise, vibration and harshness (NVH) performance of EVs. Existing gear flank modification methods apply the same modification parameters to all teeth, using a uniform amount of modification for each tooth surface. However, the effectiveness of these traditional flank modification methods has reached its limit, especially when dealing with high-speed gear pairs, where the results are not always ideal. Cattanei et al. [7] have proposed a method for reducing rotor noise by changing the spacing between circumferential blades according to a specific pattern, thereby dispersing the harmonic peak energy of blade impact frequencies and reducing the harmonic peaks of blade impact frequencies. Although the mechanism of rotor noise differs significantly from that of gear noise, this noise reduction method offers a new perspective for suppressing gear noise.

Vibration and noise reduction have always been important topics in gear design and manufacturing research [8] to [10]. For this purpose, a lot of effort has been made, among which gear flank modification is an important method for gear vibration and noise reduction [11] to [13]. Rana et al. [14] utilized a non-contact advanced precision finishing process involving pulsed electrolytic dissolution to perform five types of flank modifications and their combinations on spur gears, significantly reducing the noise and vibration of spur gears under a specific operating condition. Ghosh and Chakraborty [15] studied the influence of

*Corr. Author's Address: Central South University of Forestry and Technology, Changsha, 410004, China, zhyu@csuft.edu.cn

gear flank profile modification amount on vibration levels and identified the optimal modification amount. Through optimization, the vibrations caused by profile and pitch errors were significantly reduced. Wang [16] established the connection between gear modification, gear tooth load distribution, and the dynamic model of the gear system, and proposed a multi-objective optimization design method for helical gears that considers both vibration/noise reduction and the uniform distribution of tooth surface loads. Tang et al. [17] established a parametric model of the high-speed train traction gear transmission system and proposed a noise reduction optimization design scheme that combines tooth direction and tooth profile under multiple working conditions, achieving satisfactory transmission performance and noise reduction effects. Yoon [18] proposed a new method based on using cubic spline curves to modify the tooth profile to reduce the vibration and noise of involute gears. Li et al. [19] proposed a 3D modified tooth surface with the grinding wheel moving in an axial helical ascent and a radial parabolic motion, and established a multi-objective ant lion optimizer model to optimize the meshing performance and dynamic characteristics of the herringbone gear transmission system. Han at al. [20] proposed a method for the lead and profile modification tooth flank of the work gear by setting the movement of the A and B axes as two fourth-order polynomial functions of the axial feed of the work gear. Wang et al. [21] proposed a dual helical gear modification optimization method based on a three-segment parabolic cutter profile, which significantly reduced the vibration and noise of the gear.

In addition to the gear flank modification method, optimizing the macro geometric parameters and structural parameters of gears, as well as improving the manufacturing precision of gears, are also common methods for gear vibration and noise reduction [22] to [24]. Bozca [25] and [26] minimized torsional vibration, transmission error, and gear whine noise by optimizing the geometric parameters of the gearbox. Tang et al. [27] and [28] proposed using the minimization of noise from high-speed train traction gear transmissions as the optimization objective and obtained the optimal combination of retrofit parameters and noise data. Hou et al. [29] significantly reduced the dynamic meshing force and dynamic response of gears by optimizing the method of gear web and tooth ring thickness. Yang et al. [30] proposed the parameter optimization of weight reduction holes on gear blanks to improve the damping characteristics of lightweight gears. Xuet al. [31] studied a lightweight, low-amplitude web design method to reduce gear weight and lower noise. Qi et al. [32] employed panel acoustic contribution analysis and the response surface methodology for structural acoustic analysis and multi-objective optimization of gearboxes, aiming to reduce the radiated noise of the gearboxes.

The methods of gear flank modification, optimization of geometric and structural parameters have been proven to be effective for gear vibration and noise reduction. However, with the continuous advancement of EV technology, the requirements for gear transmission systems have gradually increased, and the existing gear vibration and noise reduction technologies and methods are gradually encountering bottlenecks. The traditional gear flank modification method, which processes all gear teeth into the same tooth surface topography, sometimes cannot achieve the ideal noise reduction effect. Inspired by Cattanei's design idea [7] of varying the spacing between blades, if the modification parameters of all gear teeth are varied according to a certain rule (such as a sine curve), creating a differentiated design in the tooth surface topography of each gear tooth, it is possible to achieve the purpose of gear pair vibration and noise reduction by tuning the fluctuations during the rotation of the gear teeth, which represents a new design approach.

To validate this innovative design approach, a mathematical model of gear tooth profile modification varying according to a sine function was established. Utilizing Adams software, the dynamic transmission characteristics of gear pairs, including centroidal angular acceleration, meshing force, and transmission error, were analyzed. Comparisons were made among unmodified, normally modified, and differentially modified gear pairs. Additionally, Simcenter 3D software was employed to compare the vibration and noise characteristics of these three sets of gear pairs. The findings demonstrated that differential modification enhances the dynamic transmission performance of gears and effectively reduces vibration and noise in gear pairs, offering a novel method for gear vibration and noise reduction. A new gear tooth modification method is proposed, in which each gear tooth is modified to different degrees and the modification amount of adjacent teeth varies according to a sine function. This method improves the dynamic transmission performance of gear pairs by introducing additional sidebands in the spectrum, thereby reducing the amplitude of the dominant gear meshing harmonics.

1 MATHEMATICAL MODEL OF GEAR TOOTH MODIFICATION PROFILE

Tooth profile modification is a primary method to avoid meshing interference and impact during tooth pair conversion, effectively reducing vibration and noise. Fig. 1 illustrates the parameter setting and modification effect of tooth profile modification. In this study, we employ an arc modification curve (radius r) for tooth profile modification, focusing on the modification of the gear top as illustrated in Fig. 1a and b. The modification begins at the intersection point C_1, where the modification start circle (radius R_1) meets the involute gear profile. The initial arc, denoted as l_1 with center O_1, passes through C_1 and reaches the top point C_2 on the gear profile. By rotating arc l_1 around C_1 by an angle $\Delta\beta$, we obtain the modified curve l_2 for the tooth top. The angle $\Delta\beta$ represents the extent of modification, and adjusting its magnitude allows for controlled modification of the tooth top, as shown in Fig. 1c. The method for modifying the tooth root is similar, as shown in Fig. 1d, and will not be elaborated further here.

Existing methods for gear modification typically standardize the modification amount or topography of all teeth on a gear, resulting in the same modification effect on all tooth surfaces. This paper introduces a differentiated modification approach, where the modification amount for each tooth on a gear varies according to a sinusoidal function. This means that the topography of each tooth is unique, thereby reducing gear vibration and noise. The modification amount for each tooth is represented by the following sinusoidal function:

$$\lambda_{(n)} = \lambda_0 + \frac{a}{2}\sin\left(\frac{2\pi}{z}n\right), \tag{1}$$

where n represents the gear tooth number, $\lambda_{(n)}$ represents the modification amount for each tooth, λ_0 is the average modification amount across all teeth, a is the threshold for modification fluctuation, and z is the number of teeth on the gear.

Due to the variability in the shape of each tooth, a separate model is established for each tooth. The following details the modeling method for the tooth profile curve during top modification. The involute parametric equation can be expressed as:

$$\begin{cases} y = R_b\cos\theta + R_b\theta\sin\theta \\ x = R_b\sin\theta - R_b\theta\cos\theta \end{cases}, \tag{2}$$

where x and y represent the coordinates of the involute in the Cartesian coordinate system, R_b is the radius of the base circle, and θ is the sum of the involute expansion angle and the pressure angle.

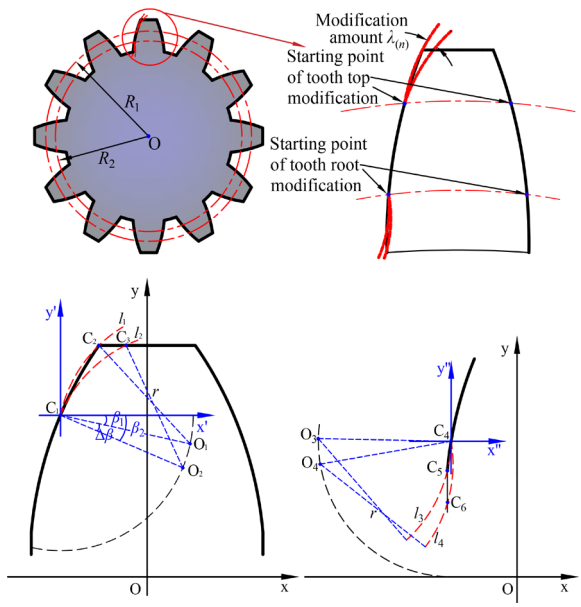

Fig. 1. *a) and b) tooth profile modification, and c) and d) coordinate system construction*

The coordinates for the starting point of the tooth top modification, $C_1(x_1, y_1)$, can be determined by solving the equations of the starting modification circle and the involute parametric equations. Similarly, the coordinates for the intersection point of the initial modification curve l_1 with the tooth top, $C_2(x_2, y_2)$, can be obtained by solving the equations for the tooth top circle and the involute. The initial modification arc l_1, passing through points C_1 and C_2 with the center at O_1, can be described by the following equation:

$$\begin{cases} (x_1 - i_1)^2 + (y_1 - j_1)^2 = r^2 \\ (x_2 - i_1)^2 + (y_2 - j_1)^2 = r^2 \end{cases}. \tag{3}$$

Here, r represents the radius of the modification arc, with the center O_1 having coordinates (i_1, j_1). A local coordinate system, $S'\{x'\ C_1\ y'\}$ is established with the modification starting point C_1 as the origin. The transformation equation between the local S′ and global coordinates $S\{x\ O\ y\}$ is as follows:

$$\begin{cases} x = x' + x_1 \\ y = y' + y_1 \end{cases}. \tag{4}$$

To transform the center O_1 from global coordinates to local coordinates O_1 (i_1', j_1'), if the angle between O_1C_1 and the x'-axis is denoted as β_1, then:

$$\begin{cases} i_1' = r\cos\beta_1 \\ j_1' = r\sin\beta_1 \end{cases}, \tag{5}$$

If the angle between O_2C_2 and the x'-axis is denoted as β_2, then:

$$\beta_2 = \beta_1 + \Delta\beta. \tag{6}$$

Here, $\Delta\beta$ is the modification amount, since each tooth has a different modification amount, so let $\Delta\beta = \lambda(n)$.

The coordinate equation of the center O_2 of the modified arc l_2 is expressed in the coordinate system S′:

$$\begin{cases} i_2' = r\cos\beta_2 \\ j_2' = r\sin\beta_2 \end{cases}. \tag{7}$$

To transform the center O_2 (i_2', j_2') from the local coordinate system S′ to the global coordinate system S as O_2 (i_2, j_2), and subsequently derive the equation of the modification arc l_2 in the global system S, which serves as the mathematical model for the tooth top modification profile, can be represented as follows:

$$\left(x_n - i_2\right)^2 + \left(y_n - j_2\right)^2 = r^2. \tag{8}$$

Here, $x_n \in (x_1, x_3)$, $y_n \in (y_1, y_3)$, $C_3(x_3, y_3)$ is the intersection of the modification arc l_2 with the tooth top circle. Collate Eqs. (4) to (7), where i_2, j_2 are respectively:

$$\begin{cases} i_2 = r\cos\left[\cos^{-1}\left(\dfrac{i_1 - x_1}{r}\right) + \lambda_{(n)}\right] + x_1 \\ j_2 = r\sin\left[\cos^{-1}\left(\dfrac{i_1 - x_1}{r}\right) + \lambda_{(n)}\right] + y_1 \end{cases}. \tag{9}$$

Similarly, the mathematical model for the tooth root modification curve can be obtained as follows:

$$\left(x_n' - i_4\right)^2 + \left(y_n' - j_4\right)^2 = r^2, \tag{10}$$

where the coordinate values i_4, j_4 of the circle center O_4 are denoted respectively:

$$\begin{cases} i_4 = r\cos\left[\cos^{-1}\left(\dfrac{i_3 - x_4}{r}\right) + \lambda'_{(n)}\right] + x_4 \\ j_4 = r\sin\left[\cos^{-1}\left(\dfrac{i_3 - x_4}{r}\right) + \lambda'_{(n)}\right] + y_4 \end{cases}. \tag{11}$$

where $x_n' \in (x_4, x_6)$, $y_n' \in (y_4, y_6)$, $C_4(x_4, y_4)$ is the starting coordinate for the tooth root modification, $C_5(x_5, y_5)$ is the intersection point of the initial modification arc l_3 with the tooth root profile, $O_3(i_3, j_3)$ is the center of the initial modification arc l_3, $O_4(i_4, j_4)$ is the center of the modification arc l_4 after a rotation angle $\lambda'_{(n)}$, where $\lambda'_{(n)}$ is the amount of tooth root modification, and $C_6(x_6, y_6)$ is the intersection point of l_4 with the tooth root profile.

2 DIFFERENTIAL MODIFICATION MODEL OF GEAR TEETH WITH SINUSOIDAL LAW

This article uses a pair of standard involute straight-tooth cylindrical gears as a case study for the following modeling and simulation. The gears have a module of 2.5 mm, a teeth number of 32:48, a pressure angle of 20°, and a tooth face width of 30 mm. Additionally, the modification arc radius is set to $r = 5$ mm, the starting radius for tooth top modification is $R_1 = 42$ mm, and the starting radius for tooth root modification is $R_2 = 38$ mm. The average amount of tooth top modification is $\lambda_0 = 8°$ with a modification differential fluctuation threshold of $a = 10°$, and the average amount of tooth root modification is $\lambda'_0 = 5°$ with a modification differential fluctuation threshold of $a' = 6°$. The parameters mentioned above were obtained after optimization, and the optimization model is shown in Fig. 2. To enhance the efficiency of modification during manufacturing, differential modification is applied only to the pinion. The amount of modification for each tooth on the pinion is set according to Eq. (1), as shown in Fig. 3, where $\lambda_{(1)}$ is the modification amount for the tooth top of the first tooth, $\lambda'_{(1)}$ is the modification amount for the tooth root of the first tooth, $\lambda_{(2)}$ is for the second tooth's top, and $\lambda'_{(2)}$ for the second tooth's root, and so on. The specific modification amounts for each tooth are shown in Table 1.

Table 1. *Setting the modification amount for each gear tooth*

Gear tooth number	Tooth top modification amount [°]	Tooth root modification amount [°]
$\lambda_{(1)}$	8+5sin(0°)=8.0000	5+3sin(0°)=5.0000
$\lambda_{(2)}$	8+5sin(11.25°)=8.9755	5+3sin(11.25°)=5.5853
$\lambda_{(3)}$	8+5sin(22.5°)=9.9134	5+3sin(22.5°)=6.1481
...	...	...
$\lambda_{(30)}$	8+5sin(326.25°)=5.2221	5+3sin(326.25°)=3.3333
$\lambda_{(31)}$	8+5sin(337.5°)=6.0866	5+3sin(337.5°)=3.8520
$\lambda_{(32)}$	8+5sin(348.75°)=7.0245	5+3sin(348.75°)=4.4147

The radius of the tooth root fillet generated by the tool is 0.8 mm. Since the tooth root fillet designed here has little influence on the meshing of gear pairs and will not interfere with the design of tooth root fillet, the existence of tooth root fillet can be ignored in the establishment of the dynamic simulation model in order to reduce simulation time. All the simulation calculations in this paper are carried out without setting the tooth root fillet, and the calculation

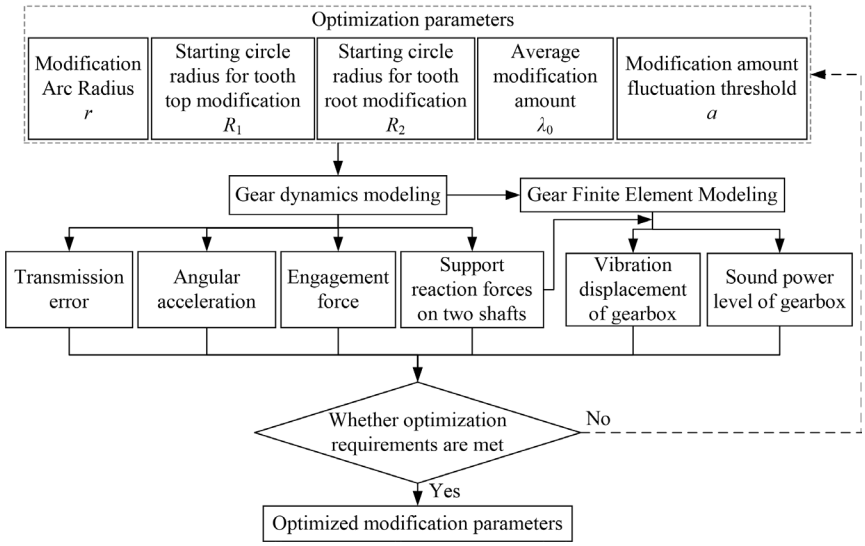

Fig. 2. *Optimization model for gear tooth modification parameters*

results are only used for comparison and analysis with each case. Using the mathematical model of the tooth profile curve described above, a differentiated tooth profile curve is established in UG software, followed by the formation of the tooth surface and three-dimensional model. The modeling process is illustrated in Fig. 4.

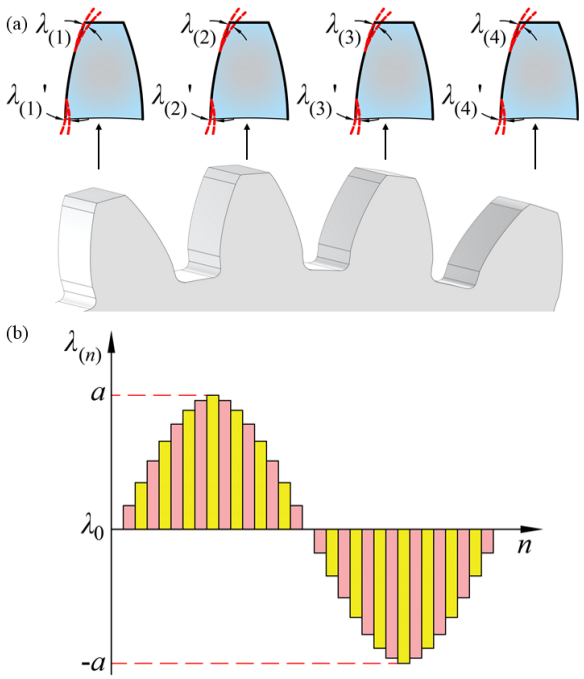

Fig. 3. *Sinusoidal design method for gear tooth modification amounts, a) Gear tooth modification amount arrangements, b) Change rule of gear tooth modification amounts*

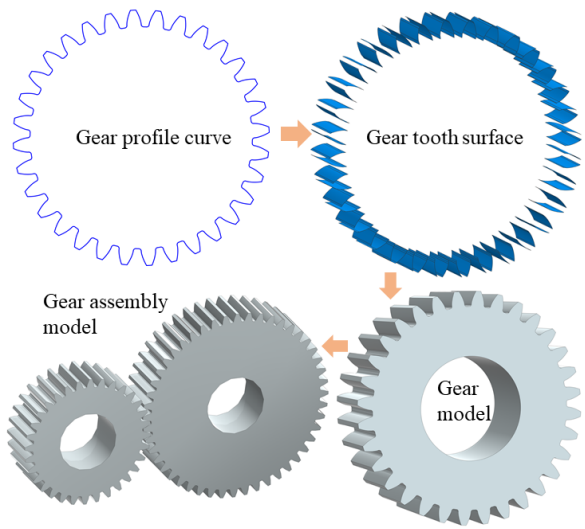

Fig. 4. *Establishing the 3D model process for gear pairs*

3 SIMULATION AND ANALYSIS OF GEAR DYNAMICS PERFORMANCE

3.1 Establishment of Gear Dynamics Model

The gear model assembled in UG will be imported into Adams software for multibody dynamics simulation, the construction of the gear dynamics model is shown in Fig. 5. The material and contact parameters of the gear pair are set as shown in Table 2. During the simulation process, the step function is used to define the speed of the driving gear (pinion) to the corresponding value within 0-0.1 s, and the driven gear (gear) is also subjected to a torque load to the

corresponding value. The values are kept constant for solving calculations within 0.1 s to 1 s.

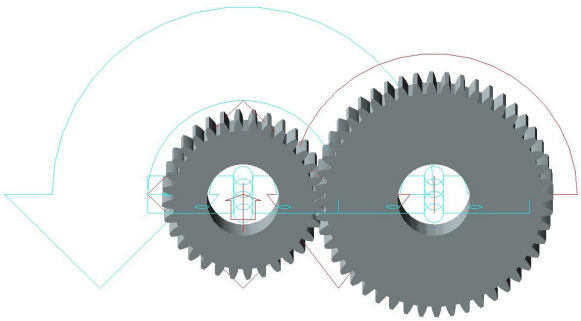

Fig. 5. *Gear dynamics modeling*

Table 2. *Parameterization of dynamic model simulation*

Parameter	Value
Stiffness [N/mm]	8×10^5
Coefficient of static friction	0.3
Power index [-]	1.5
Static translation coefficient [mm/s]	100
Damping [N·s/mm]	10
Coefficient of kinetic friction [-]	0.1
Depth of penetration [mm]	0.1
Friction translation coefficient [mm/s]	1000

To verify and analyze the transmission performance of the differentiated profile modification gear pair, four pairs of gears are designed with the same geometric parameters. The first pair of gears does not undergo tooth profile modification, the second and the third pairs of gears adopts the existing common gear modification method, and the same amount of modification is applied to the tooth flanks of both the pinion and gear. The fourth pair of gears adopt the design method of differentiated modification, and their modification parameters are shown in Table 3. The differentiated modification parameters of the fourth pair of gears were obtained through the optimization model shown in Fig. 2. The modification method is the same for Case 2 and Case 3. The tooth top in Case 2 is modified by 8° and the tooth root by 5°, while the tooth top in Case 3 is modified by 13° and the tooth root by 8°, which is the same amount of modification for each tooth in these two sets of cases. The dynamic meshing performance of the gear pair during transmission is analyzed by simulating the centroid angle acceleration of the driven gear and the meshing force of the gear pair under the conditions of the driven gear load being 100 N·m and 350 N·m respectively, and the driving gear speed is 3000 rpm, 5000 rpm, and 8000 rpm, respectively.

Table 3. *Pinion parameters for tooth profile modification*

	Mean value of modification amount [°]		Fluctuation threshold of modification amount [°]	
	Top	Root	Top	Root
Case 1	0	0	0	0
Case 2	8	5	0	0
Case 3	13	8	0	0
Case 4	8	5	10	6

3.2 Comparative Analysis of Gear Angular Acceleration

The angular acceleration of the driven gear's centroid was measured over time using simulation, and its frequency domain representation was obtained through Fourier transformation. Due to space limitations, only the frequency domain graphs are shown here, and subsequent analyses will follow this format.

From the comparative analysis of gear angular acceleration in Figs. 6 to 11:

1. The theoretical meshing frequencies at known speeds of 3000 rpm, 5000 rpm, and 8000 rpm are respectively 1600 Hz, 2666.67 Hz, and 4266.67 Hz. The meshing frequencies in all spectral graphs correspond to the theoretical values, confirming the accuracy of the dynamic model.

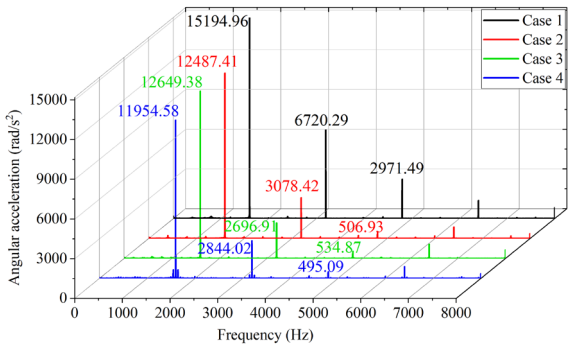

Fig. 6. *Comparison of angular acceleration spectrograms at 3000 rpm and 100 N·m*

2. Under the same speed, the amplitude of angular acceleration at 1 to 3 times the meshing frequency increases with higher loads, under the same load, the amplitude generally tends to increase with higher speeds.
3. Across all conditions, the amplitude of angular acceleration at the fundamental meshing frequency is highest for Case 1, followed by Case 2 and Case 3, and lowest for Case 4. This indicates that differentiated modification results in lower angular accelerations compared to traditional modified and unmodified gears, with

the greatest reduction at 5000 rpm of 100 Nm, where Case 4 is reduced by 27.74 % compared to Case 1, 9.28 % compared to Case 2 and 10.75 % compared to Case 3.

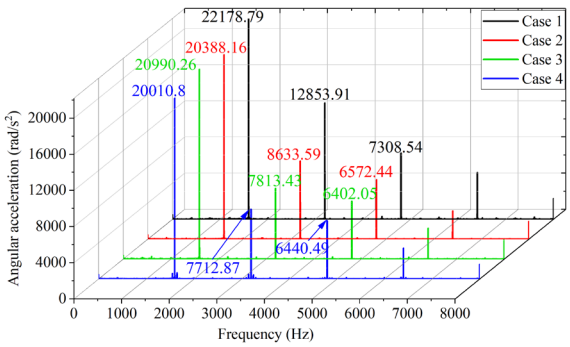

Fig. 7. *Comparison of angular acceleration spectrograms at 3000 rpm and 350 N·m]*

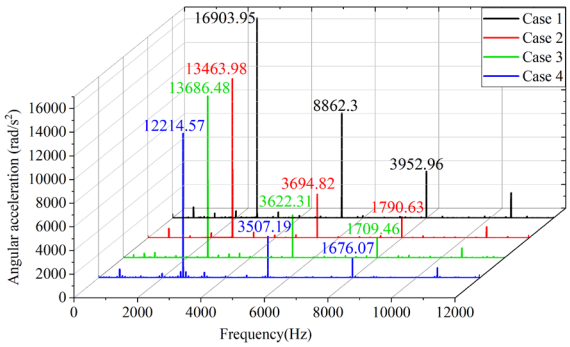

Fig. 8. *Comparison of angular acceleration spectrograms at 5000 rpm and 100 N·m*

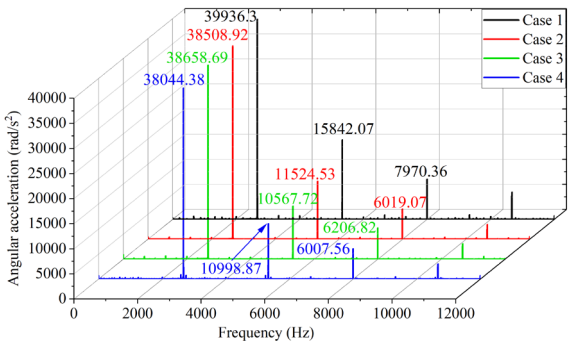

Fig. 9. *Comparison of angular acceleration spectrograms at 5000 rpm and 350 N·m*

4. At twice and three times the meshing frequency, Case 1 also shows the highest amplitude, followed by Case 2 and Case 3, and Case 4 the lowest. At twice the meshing frequency, the maximum reductions for Case 4 compared to Cases 1 to 3 are 60.43 %, 10.66 % and 4.35 % respectively, under conditions of 5000 rpm of 100 Nm, 3000 rpm of 350 Nm and 8000 rpm of 100 Nm. At three times the meshing frequency, the maximum reductions for Case 4 compared to Cases 1 to 3 are 57.6 %, 7.08 % and 3.21 %, respectively.
5. Compared to gears modified by traditional methods, the amplitude of angular acceleration of the driven gear's centroid is reduced, indicating that differentiated modification methods are beneficial in reducing vibration and noise in gear pairs.
6. Compared to Cases 1 to 3, Case 4 shows varying degrees of increase in the amplitude of sidebands adjacent to the meshing frequency peaks, proving the correctness of the method proposed in this paper, which involves introducing additional sidebands to reduce the amplitude of gear meshing harmonics.

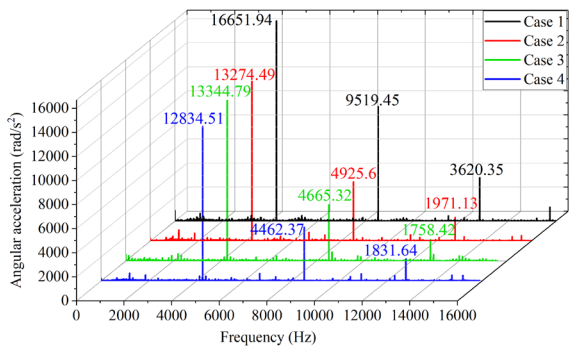

Fig. 10. *Comparison of angular acceleration spectrograms at 8000 rpm and 100 N·m*

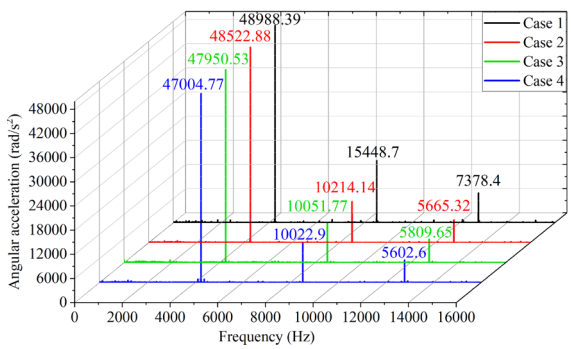

Fig. 11. *Comparison of angular acceleration spectrograms at 8000 rpm and 350 N·m*

7. To ensure the accuracy and reliability of the results, angular acceleration data from 80 different operational conditions were analyzed, with sampling conducted across a range of speeds from 1000 rpm to 10000 rpm and loads from 50

N·m to 400 N·m. A detailed comparison revealed that in these 80 conditions, compared to Case 1, Case 4 demonstrated a reduction in the amplitude of the first three meshing frequencies in 79 cases, achieving an effectiveness rate of 98.75 %. When compared to Case 2, the effectiveness rate reached 71.25 %. This data robustly supports the superior dynamic performance of differentially modified gear teeth over conventionally modified gear teeth.

3.3 Comparative Analysis of Engagement Force

Through simulation measurements, the resultant forces in the x and y directions during the meshing of the driving and driven gears were plotted over time, and their frequency domain graphs were obtained through Fourier transformation. At the initial stage of gear meshing, due to the impact between the teeth, a large meshing force is generated. However, this stage has a minor impact on the overall analysis and can be disregarded .

From the comparative analysis of gear meshing forces in Fig. 12 to 17:

1. At the same speed, the amplitude of the meshing force at harmonic frequencies increases with higher loads, at the same load, the amplitude of the meshing force at harmonic frequencies generally tends to increase with higher speeds.
2. Across all conditions, the amplitude of the meshing force at the fundamental meshing frequency is highest for Case 1, followed by Case 2 and Case 3, and lowest for Case 4. This indicates that the meshing force for differentially modified gears is lower than that for traditionally modified and unmodified gears. At the condition of 5000 rpm and 100 N·m, the reduction reaches its maximum value, with Case 4 showing a decrease of 27.92 % compared to Case 1, 9.14 % compared to Case 2 and 10.37 % compared to Case 3.
3. The same trend is observed at the second and third harmonic frequencies, where Case 1 has the highest amplitude, followed by Case 2 and Case 3, and Case 4 has the lowest. At the second harmonic frequency, Case 4 shows the maximum reduction compared to Cases 1-3 at conditions of 5000 rpm of 100 N·m, 3000 rpm of 350 Nm and 8000 rpm of 100 Nm, with maximum reductions of 59.24 %, 10.43 % and 4.63 %, respectively. At the third harmonic frequency, the maximum reductions for Case 4 compared to Cases 1 to 3 are 80.38 %, 6.74 % and 9.07 %, respectively.
4. Compared to traditionally modified gears, the amplitude of the meshing force of the driven gear is reduced in Case 4, indicating that differential modification methods are beneficial in reducing vibration and noise in gear pairs.
5. Compared to Cases 1 to 3, Case 4 also shows varying degrees of increase in the amplitude of sidebands around the peaks of meshing harmonics, which is beneficial for reducing the amplitude at these harmonic frequencies.

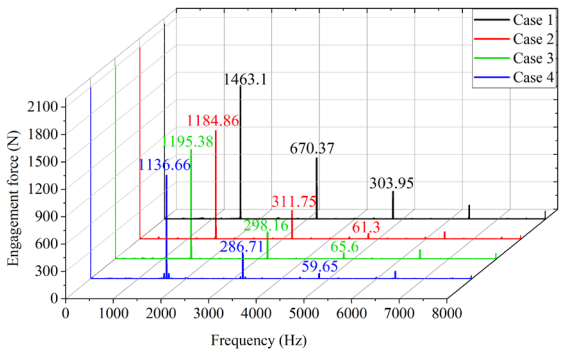

Fig. 12. *Comparison of engagement force spectrograms at 3000 rpm and 100 N·m*

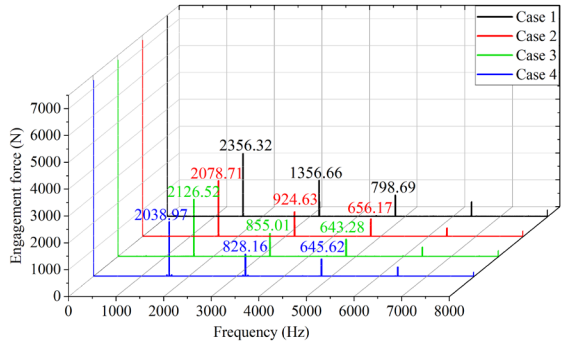

Fig. 13. *Comparison of engagement force spectrograms at 3000 rpm and 350 N·m*

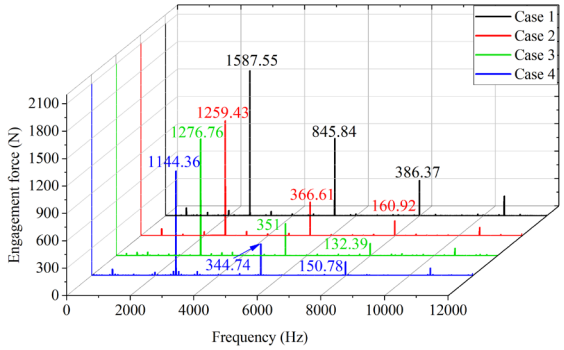

Fig. 14. *Comparison of engagement force spectrograms at 5000 rpm and 100 N·m*

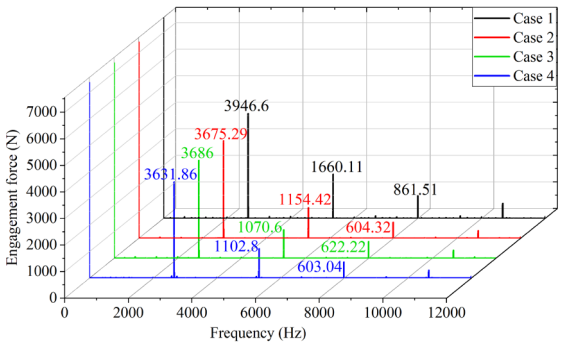

Fig. 15. *Comparison of engagement force spectrograms at 5000 rpm and 350 N·m*

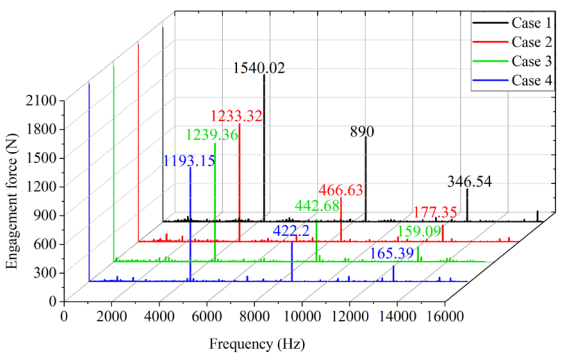

Fig. 16. *Comparison of engagement force spectrograms at 8000 rpm and 100 N·m*

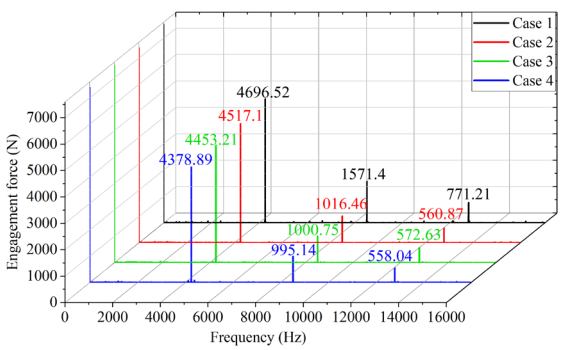

Fig. 17. *Comparison of engagement force spectrograms at 8000 rpm and 350 N·m*

3.4 Comparative Analysis of Gear Transmission Errors

Through gear dynamics simulation, transmission error curves of gear pairs can be obtained, because transmission error is independent of gear speed, and since the dynamics model uses rigid bodies for simulation, transmission error is also unaffected by load. It only analyzes the transmission error under one operating condition (5000 rpm and 100 N·m) for comparison, as shown in Fig. 18. Fast Fourier Transform (FFT) of these transmission errors yields the order spectra, as illustrated in Fig. 19. From the comparative analysis of the gear transmission errors in Fig. 18 and 19, it can be observed that:

1. The driven gear exhibits 48 cycles of fluctuation per revolution, aligning with the number of teeth on the driven gear. Unlike Case 1, Case 2 and Case 3, Case 4's transmission error curve is not stable but matches the pattern of a complete sinusoidal cycle. This phenomenon confirms the accuracy of the differentiated gear modification model.

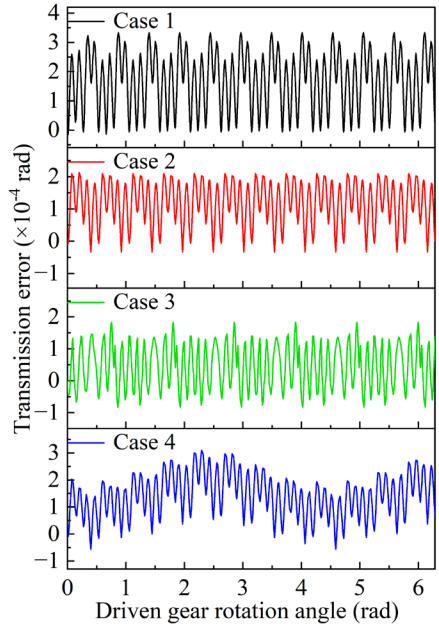

Fig. 18. *Comparison of transmission error time domain diagrams*

2. The opening sizes of the transmission error curves in all Cases are comparable, and the periodic patterns are consistent. By comparing the amplitude of fluctuations in the transmission error curves, Case 1 has the largest, followed by Case 2 and Cases 3, and Case 4 has the smallest, indicating that the meshing in Case 4 is the most stable.
3. The sum of the amplitudes of the first four orders of transmission errors is the largest in Case 1, followed by Case 2 and Cases 3, and the smallest in Case 4. The sum of the amplitudes of the first four orders of transmission errors effectively reflects the quality of the gear profile modification [33]. Case 4 shows a reduction of 38.89 % compared to Case 1, 15.79 % compared to Case 2 and 25.74 % compared to Case 3. This demonstrates that differentiated modification

provides smoother transmission compared to traditional modification methods and unmodified gears.

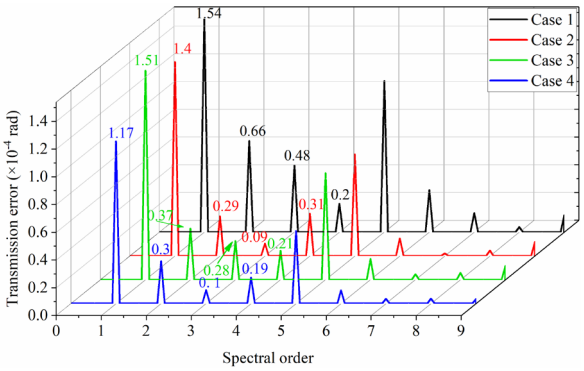

Fig. 19. *Comparison of transmission error spectrum diagrams*

4 SIMULATION AND ANALYSIS OF GEARBOX VIBRATION AND RADIATED NOISE

4.1 Establishment of Gearbox Finite Element Model

The excitations generated during the gear meshing process are transmitted through the gear shafts to the gearbox, causing vibrations and noise in the gearbox. Therefore, the following will simulate the noise of the gear pair based on the finite element method. In the pre-processing module, the gearbox is meshed, and its material is specified as gray cast iron. In Adams software, the support reaction data in the x and y directions of the gear pair's shafts are extracted, these support reaction data are used as the excitation source for vibration response analysis of the gearbox, and the radiated noise of the gearbox are solved. In Simcenter 3D software, corresponding models for acoustic analysis of the gearbox are established. The thickness of the gearbox is 8 mm, the radius of the sound field is 1 m.

Table 4. *Partial natural frequency of gearbox*

Spectral order	Natural frequency [Hz]	Spectral order	Natural frequency [Hz]
6	2008	42	6393
15	3186	44	6525
29	5074	47	6977
30	5190	50	7335
55	6051	62	8035

Since this article only compares the impact of different cases on the vibration and noise of the gearbox, to prevent other factors from affecting the comparison results, the entire bottom of the gearbox is securely constrained. Modal analysis is performed on the gearbox to solve the first 100 modes of the gearbox and obtain its first 100 natural frequencies. As shown in Table 4, due to space limitations, only the natural frequencies of the gearbox that have a significant impact on subsequent simulation analysis are listed.

4.2 Comparative Analysis of Gearbox Sound Power Levels

From the comparative analysis of the sound power levels of the gearbox casing shown in Figs . 20 to 25, the following can be observed:

1. At the same rotational speed, the sound power level amplitudes at the first three meshing frequencies increase with higher loads. Due to the influence of the casing's natural frequencies, resonance occurs at frequencies close to the natural frequencies of the casing, resulting in larger amplitudes near these natural frequencies. For example, near the frequency of 2008 Hz, an increase in amplitude is observed in all conditions, especially at a rotational speed of 5000 rpm. Increased amplitudes are also seen between frequencies of 6000 Hz to 8000 Hz. Additionally, at a rotational speed of 3000 rpm, the amplitude at twice the meshing frequency is higher than at the meshing frequency, and at rotational speeds of 5000 rpm and 8000 rpm, the amplitude at three times the meshing frequency is higher than at twice the meshing frequency due to this reason.

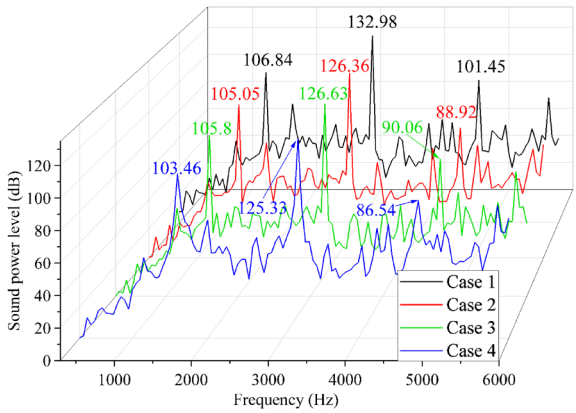

Fig. 20. *Comparison of sound power level spectrograms at 3000 rpm and 100 N·m*

2. Under all conditions, the sound power level amplitude at the meshing frequency is the highest for Case 1, followed by Case 2 and Case 3, and the lowest for Case 4. The maximum reduction

is observed at conditions of 3000 rpm of 350 Nm and 5000 rpm of 350 Nm, where Case 4 is reduced by 3.43 % compared to Case 1, 2.43 % compared to Case 2 and 2.47 % compared to Case 3.

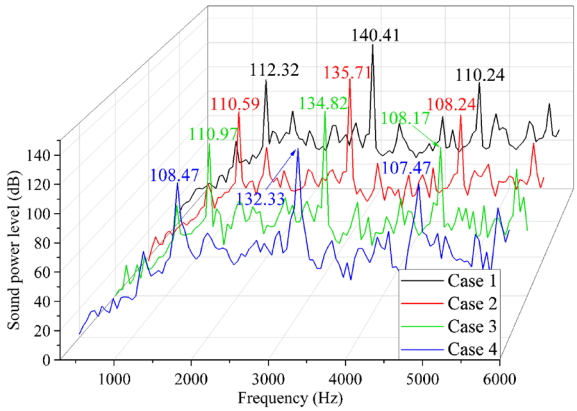

Fig. 21. *Comparison of sound power level spectrograms at 3000 rpm and 350 N·m*

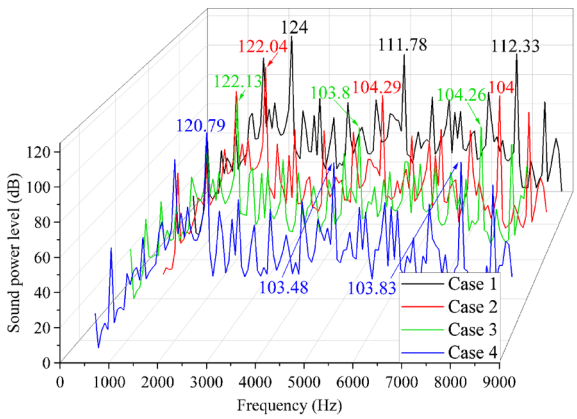

Fig. 22. *Comparison of sound power level spectrograms at 5000 rpm and 100 N·m*

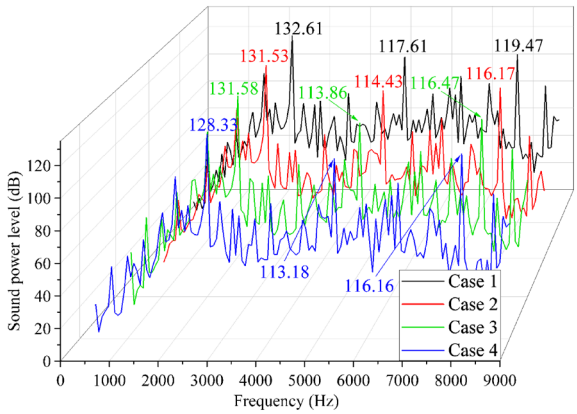

Fig. 23. *Comparison of sound power level spectrograms at 5000 rpm and 350 N·m*

3. At twice and three times the meshing frequency, Case 1 also shows the highest amplitude, followed by Case 2 and Case 3, and the lowest for Case 4. At twice the meshing frequency, the maximum reduction for Case 4 compared to Cases 1-3 occurs at conditions of 5000 rpm of 100 Nm and 3000 rpm of 350 Nm, with maximum reductions of 7.43 %, 2.49 % and 1.85 %, respectively. At three times the meshing frequency, the maximum reductions for Case 4 compared to Cases 1 to 3 are 14.7 %, 2.68 % and 3.91 %, respectively.

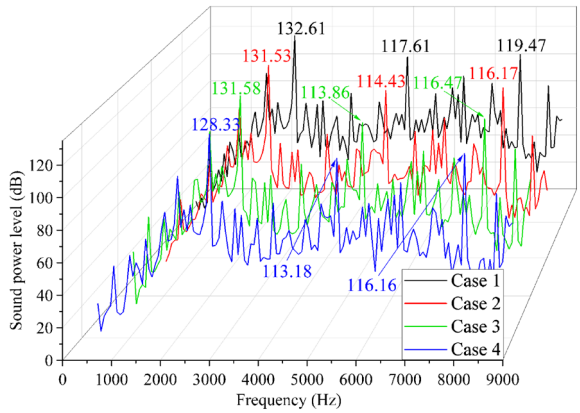

Fig. 23. *Comparison of sound power level spectrograms at 5000 rpm and 350 N·m*

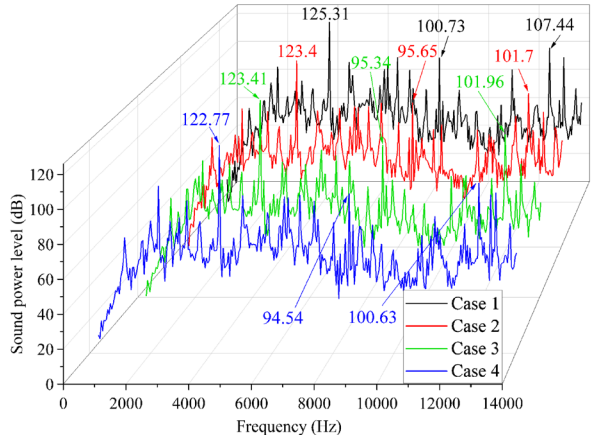

Fig. 24. *Comparison of sound power level spectrograms at 8000 rpm and 100 N·m*

4. All of these laws are similar to the laws of vibration displacement, illustrating the close correlation between vibration and noise. Compared to gears modified by traditional methods, the sound power level amplitudes of the driven gear are reduced, indicating that differentiated modification methods are beneficial in reducing the noise of gear pairs.

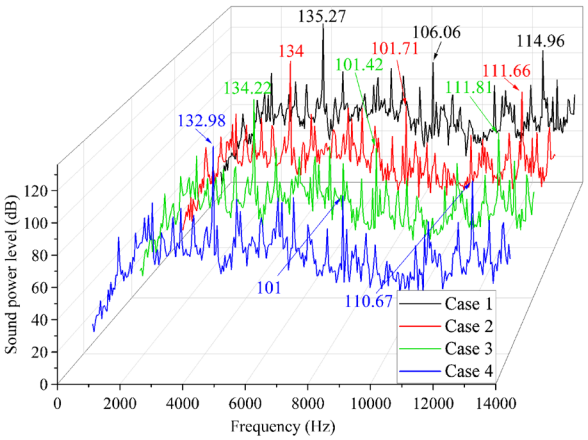

Fig. 25. *Comparison of sound power level spectrograms at 8000 rpm and 350 N·m*

5 CONCLUSIONS

This paper discusses the impact of using a differentiated tooth modification method on the dynamic meshing performance of gear pairs. It compares this method with normal tooth modification gears and unmodified gears, arriving at the following main conclusions:

1. A differentiated tooth modification method is proposed, where the modification amount of adjacent teeth varies according to a sine function, and a mathematical model of the gear tooth profile is established.
2. Using transmission error, centroid angular acceleration, and meshing force to characterize the dynamic meshing performance of gear pairs, a comparative analysis is conducted between gears using the differentiated modification method, normally modified gears, and unmodified gears. The results show that differentiated modification can improve the dynamic meshing performance of gear pairs. Compared to normally modified gears, the sum of the amplitudes of the first four orders of transmission error is reduced by up to 25.74 %, the amplitude of the angular acceleration at the meshing frequency is reduced by up to 10.75 %, and the amplitude of the meshing force at the meshing frequency is reduced by up to 10.37 %.
3. A comparative analysis of the noise conditions of three pairs of gears shows that, compared to normally modified gears, the sound power level amplitude at the meshing frequency is reduced by up to 2.47 %.
4. Eighty sets of conditions were sampled for multibody dynamics analysis, and the simulation results show that gears with differentiated modification performed better in dynamic meshing performance in over 70 % of the conditions compared to normally modified gears, fully validating the effectiveness of the differentiated modification method in reducing vibration and noise.

6 ACKNOWLEDGMENTS

The research was supported by the Natural Science Foundation of Hunan Province (2024JJ5643 and 2022JJ40876), the National Natural Science Foundation of China (U22B2084), the Hunan Provincial Key R&D Program (2023GK2053).

7 REFERENCES

[1] Yang, J.-x., Chen, Z.-y., Shi, W.-k., Yuan, R.-f., Liu, J., Zhao, Y.-y. (2023). Vibration control of commercial vehicle drive axles based on modification of helical gears. *Mechanical Systems and Signal Processing*, vol. 193, 110252, **DOI:10.1016/j.ymssp.2023.110252**.

[2] Zhongxing, L., Ni, S., Guangping, W. (2011). Experimental study on vibration and noise of pure electric vehicle (PEV) drive system. *2011 International Conference on Electric Information and Control Engineering*, p. 5914-5917, **DOI:10.1109/iceice.2011.5776874**.

[3] Behvar, A., Tahmasbi, K., Savich, W., Haghshenas, M. (2024). Tooth interior fatigue fracture in automotive differential gears. *Engineering Failure Analysis*, vol. 156, p. 107829, **DOI:10.1016/j.engfailanal.2023.107829**.

[4] Stadtfeld, H.J. (2020). Introduction to electric vehicle transmissions. *Gear Technology*, p. 42-50.

[5] Stadtfeld, H.J. (2021). Drive concepts using super reduction hypoids combined with cylindrical gear reductions. *Gear Technology*, p. 46-53.

[6] Stadtfeld, H.J. (2020). *EDrive Transmission Guide: New Solutions for Electric and Hybrid Vehicle Transmissions*. Gleason Works, Rochester.

[7] Cattanei, A., Ghio, R., Bongiov, A. (2007). Reduction of the tonal noise annoyance of axial flow fans by means of optimal blade spacing. *Applied Acoustics*, vol. 68, no. 11-12, p. 1323-1345, **DOI:10.1016/j.apacoust.2006.07.012**.

[8] Sun, M., Lu, C., Liu, Z., Sun, Y., Chen, H., Shen, C. (2020). Classifying, predicting, and reducing strategies of the mesh excitations of gear whine noise: A survey. *Shock and Vibration*, vol, 2020, 9834939, **DOI:10.1155/2020/9834939**.

[9] Son, G.-H., Kim, B.-S., Cho, S.-J., Park, Y.-J. (2020). Optimization of the housing shape design for radiated noise reduction of an agricultural electric vehicle gearbox. *Applied Sciences*, vol. 10, no. 23, 8414, **DOI:10.3390/app10238414**.

[10] Wang, Z., Jiao, Y., Chen, Z., Qu, X., Fu, T. (2021). An analytical study of average radiation efficiency of rotating annular plates in rotating frame. *Applied Acoustics*, vol. 174, p. 107786, **DOI:10.1016/j.apacoust.2020.107786**.

[11] Andary, F., Heinzel, C., Wischmann, S., Berroth, J., Jacobs, G. (2023). Calculation of tooth pair stiffness by finite element

analysis for the multibody simulation of flexible gear pairs with helical teeth and flank modifications. *Multibody System Dynamics*, vol. 59, no. 4, p. 395-428, **DOI:10.1007/s11044-023-09926-4**.

[12] Tang, Z., Wang, M., Chen, Z., Sun, J., Wang, M., Zhao, M. (2020). Design of multi-stage gear modification for new energy vehicle based on optimized bp neural network. *IEEE Access*, vol. 8, p. 199034-199050, **DOI:10.1109/access.2020.3035570**.

[13] Mohamad, E.N., Komori, M., Matsumura, S., Ratanasumawong, C., Yamashita, M., Nomura, T., Houjoh, H., Kubo, A. (2010). Effect of variations in tooth flank form among teeth on gear vibration and an sensory evaluation method using potential gear noise. *Journal of Advanced Mechanical Design Systems and Manufacturing*, vol. 4, no. 6, p. 1166-1181, **DOI:10.1299/jamdsm.4.1166**.

[14] Rana, V., Jain, N.K., Pathak, S. (2023). Improving functional performance characteristics of spur gears through flank modifications by non-contact advanced finishing process. *International Journal of Advanced Manufacturing Technology*, vol. 124, p. 1787-1811, **DOI:10.1007/s00170-022-10566-9**.

[15] Ghosh, S.S., Chakraborty, G. (2016). On optimal tooth profile modification for reduction of vibration and noise in spur gear pairs. *Mechanism and Machine Theory*, vol. 105, p. 145-163, **DOI:10.1016/j.mechmachtheory.2016.06.008**.

[16] Wang, C. (2021). Multi-objective optimal design of modification for helical gear. *Mechanical Systems and Signal Processing*, vol. 157, 107762, **DOI:10.1016/j.ymssp.2021.107762**.

[17] Tang, Z., Lu, M., Wang, M., Sun, J. (2024). Research on modification and noise reduction optimization of electric multiple units traction gear under multiple working conditions. *Plos One*, vol. 19, no. 2, p. e0298785, **DOI:10.1371/journal.pone.0298785**.

[18] Yoon, K. (1993). *Analysis Of Gear Noise And Design For Gear Noise Reduction*, Purdue University, West Lafayette.

[19] Li, Z., Wang, S., Li, F., Li, L., Zou, H., Liu, L. (2022). Research on multiobjective optimization design of meshing performance and dynamic characteristics of herringbone gear pair under 3D modification. *Journal of Mechanical Design*, vol. 144, no. 10, p. 103401, **DOI:10.1115/1.4054809**.

[20] Han, J., Zhu, Y., Xia, L., Tian, X. (2018). A novel gear flank modification methodology on internal gearing power honing gear machine. *Mechanism and Machine Theory*, vol. 121, p. 669-682, **DOI:10.1016/j.mechmachtheory.2017.11.024**.

[21] Wang, C., Cui, H.Y., Zhang, Q.P., Wang, W.M. (2016). Modified optimization and experimental investigation of transmission error, vibration and noise for double helical gears. *Journal of Vibration and Control*, vol. 22, no. 1, p. 108-120, **DOI:10.1177/1077546314525216**.

[22] Li, F., Qin, Y., Ge, L., Pang, Z., Liu, S., Lin, D. (2015). Influences of planetary gear parameters on the dynamic characteristics - a review. *Journal of Vibroengineering*, vol. 17, no. 2, p. 574-586.

[23] Raut, A.S., Khot, S.M., Salunkhe, V.G. (2024). Optimization of geometrical features of spur gear pair teeth for minimization of vibration generation. *Journal of Vibration Engineering & Technologies*, vol. 12, p. 533-545, **DOI:10.1007/s42417-023-00857-0**.

[24] Younes, E.B., Changenet, C., Bruyère, J., Rigaud, E., Perret-Liaudet, J. (2022). Multi-objective optimization of gear unit design to improve efficiency and transmission error. *Mechanism and Machine Theory*, vol. 167, 104499, **DOI:10.1016/j.mechmachtheory.2021.104499**.

[25] Bozca, M. (2018). Transmission error model-based optimisation of the geometric design parameters of an automotive transmission gearbox to reduce gear-rattle noise. *Applied Acoustics*, vol. 130, p. 247-259, **DOI:10.1016/j.apacoust.2017.10.005**.

[26] Bozca, M. (2010). Torsional vibration model based optimization of gearbox geometric design parameters to reduce rattle noise in an automotive transmission. *Mechanism and Machine Theory*, vol. 45, no. 11, p. 1583-1598, **DOI:10.1016/j.mechmachtheory.2010.06.014**.

[27] Tang, Z., Wang, M., Xiong, X., Wang, M., Sun, J., Yan, L. (2020). Optimal design of noise reduction and shape modification for traction gears of EMU based on improved BP neural network. *Noise Control Engineering Journal*, vol. 69, no. 4, p. 373-388, **DOI:10.3397/1/376934**.

[28] Tang, Z., Wang, M., Hu, Y., Mei, Z., Sun, J., Yan, L. (2020). Optimal design of traction gear modification of high-speed EMU based on radial basis function neural network. *IEEE Access*, vol. 8, p. 134619-134629, **DOI:10.1109/access.2020.3007449**.

[29] Hou, L., Lei, Y., Fu, Y., Hu, J. (2020). Effects of lightweight gear blank on noise, vibration and harshness for electric drive system in electric vehicles. *Proceedings of The Institution of Mechanical Engineers Part K-Journal of Multi-body Dynamics*, vol. 234, no. 3, p. 447-464, **DOI:10.1177/1464419320915006**.

[30] Yang, J., Zhang, Y., Lee, C.-H. (2022). Multi-parameter optimization-based design of lightweight vibration-reduction gear bodies. *Journal of Mechanical Science and Technology*, vol. 36, p. 1879-1887, **DOI:10.1007/s12206-022-0325-1**.

[31] Xu, G., Dai, N., Tian, S. (2021). Principal stress lines based design method of lightweight and low vibration amplitude gear web. *Mathematical Biosciences and Engineering*, vol. 18, no. 6, p. 7060-7075, **DOI:10.3934/mbe.2021351**.

[32] Qi, L., Zhou, J., Xu, H. (2022). Multi-objective optimization of gearbox based on panel acoustic participation and response surface methodology. *Journal of Low Frequency Noise Vibration and Active Control*, vol. 41, no. 3, p. 1108-1130, **DOI:10.1177/14613484221091075**.

[33] R. Li, Wang, J. (1997). Gear system dynamics - vibration, impact, noise. Science Press, Beijing (in Chinese).